International Journal of
Energy & Technology
www.journal-enertech.eu

ISSN 2035-911X

International Journal of Energy & Technology 3 (2) (2011) 1–13

FREE CONVECTION IN A VERTICAL DOUBLE PASSAGE WAVY CHANNEL FILLED WITH A WALTERS FLUID (MODEL B')

J. Prathap Kumar[*,1], J.C. Umavathi[*,1], Ali J. Chamkha[**] and H. Prema[*,3]

[*]Department of Mathematics, Gulbarga University, Gulbarga 585 106, Karnataka, India
p_rthap@yahoo.com[1], jc_uma11@yahoo.com[2], ashkptl@rediff.com[3]

[**]Manufacturing Engineering Department, The Public Authority for Applied Education and Training, Shuweikh 70654, Kuwait, achamkha@yahoo.com

ABSTRACT

The present analysis is concerned with the flow characteristics of fully developed free convection flow of a Walters fluid (Model B') in a vertical channel divided into two passages (by means of a baffle) for two separate flow streams. Each stream has its own individual velocity and temperature fields. One of the walls of the channel is wavy while the other is flat and both walls are maintained at constant but different temperatures. The coupled non-linear partial differential equations governing the fluid motion in the channel have been solved by a linearization technique wherein the flow is assumed to consist of two parts; a mean part and a perturbed part. Exact solutions are obtained for the mean part and a perturbed part is solved using a long wave approximation. The velocity and temperature values are obtained and discussed for the various physical parameters such as the Grashof number, wall temperature ratio, viscoelastic parameter and λx at different positions of the baffle. The variation of the skin friction and the Nusselt number are given in tables for different governing parameters. It is found that the viscoelastic parameter, wave number and the amplitude parameter reduce the skin friction at the wavy wall while it remains invariant at the flat wall. In addition, the effect of wave number is found to decrease the rate of heat transfer at the wavy wall and increase at the flat wall.

Keywords: Wavy vertical channel, baffle, Walters fluid

1. INTRODUCTION

The prediction of heat transfer from irregular surfaces is a topic of fundamental importance for some heat transfer devices, such as, flat plate solar collectors, flat plate condensers in refrigerators, double-wall thermal insulation, underground cable systems, electric machinery, cooling system of micro-electronic devices, natural circulation in the atmosphere, the molten core of the Earth, etc. In addition, roughened surfaces could be used in the cooling of electrical and nuclear components where the wall heat flux is known. Surfaces are sometimes intentionally roughened to enhance heat transfer. Process involving heat and mass transfer are often encountered in the chemical industry, in reservoir engineering connection with thermal recovery processes, and in the study of the dynamics of salty hot springs in the sea. In view of these applications, several authors have made investigations of the fluid flows over a wavy wall. Vajravelu and Sastri [1] have made an interesting analysis of the free convective heat transfer in a viscous incompressible fluid bounded by a long (when compared with the width of the channel) vertical wavy and a parallel flat wall. Later, Vajravelu [2] studied the combined free and forced convection in hydrodynamic flows in a vertical wavy channel with traveling thermal waves. Malashetty et al. [3] studied on magneto convective flow and heat transfer between vertical wavy wall and a parallel flat wall. Srinivas and Muthuraj [4] studied MHD flow with slip effects and temperature-dependent heat source in a vertical wavy porous space.

It is necessary to study the heat transfer for more complex geometries because the prediction of heat transfer for irregular surfaces is a topic of great importance and irregular surfaces often occur in many applications. Recently several studies by Rathish Kumar et al. [5,6], Murthy et al. [7] and Kumar and Shalini [8] have been reported and were concerned with natural convection heat transfer in wavy vertical porous enclosures.

It is now generally recognized that in industrial applications non-Newtonian fluids are more appropriate than Newtonian fluids. Numerous models were suggested for non-Newtonian fluids with their constitutive equations varying greatly in complexity. Already the class of flows for which an exact solutions is possible for Navier-Stokes equations that govern the flow of Newtonian fluids is rather restricted. This class further narrowed down for non-Newtonian fluids on account of the non-linear relationship between the stress and rate of strain at any point of the flow. Rheological properties of materials are specified in general by their real fluids especially those with low molecular weight, is described by Navier-Stokes theory. There are many complex fluids such as polymer solutions, soaps, blood, paints, certain oils and greases which are not well described by a Newtonian constitutive equation.

Among the many models which have been used to describe the non-Newtonian behavior exhibited by these, fluids, the fluids of differential type (Dunn and Rajagopal [9]) and those of rate type (Rajagopal [10]) have received much attention.

The rate of heat transfer in a vertical channel could be enhanced by using special inserts. These inserts can be specially designed to increase the included angle between the velocity vector and the temperature gradient vector, rather than to promote turbulence. This increases the rate of heat transfer without a considerable drop in the pressure (Guo and Wang [11]). A plane baffle may be used as an insert to enhance the rate of heat transfer in the channel. To avoid a considerable increase in the transverse thermal resistance into the channel, a thin and perfectly conductive baffle is used.

To the present authors knowledge, all published heat transfer convection studies in the vertical channel are concerned with single-passage channels (references [12-20]). Therefore, the purpose of this paper is to study analytically the free convection of a Walters fluid (model B') in a vertical wavy double passage channel.

2. Mathematical formulation

Consider a steady two dimensional laminar free convection Walter's fluid flow in an open-ended vertical channel with one wavy wall and another flat wall as shown in Fig. 1. The channel is divided into two passages by means of a perfectly conducting thin baffle, for which the transverse thermal resistance can be neglected (Cheng et al. [21] and Salah El-Din [22, 23]). The X axis is taken upwards and parallel to the flat wall, while the Y-axis is taken perpendicular to it in such a way that the wavy wall is represented by $Y = \varepsilon^* \cos(kX)$ and the flat wall by $Y = d$. The wavy and flat walls are maintained at a constant temperature T_w and T_1, respectively. The following assumptions are made:

a. All fluid properties are constant except the density in the buoyancy force.
b. The dissipative effects and the work of deformation are neglected in the energy equation.
c. The wavelength of the wavy wall is large compared with the breadth of the channel.
d. For fully developed flow, it is assumed that the transverse velocity and temperature gradient in the axial direction are zero.

The boundary conditions relevant to the problem are taken as,

$$\begin{aligned} &U_1 = V_1 = 0, \qquad T_1 = T_w \quad \text{on } Y = \varepsilon^* \cos(kX) \\ &\left.\begin{aligned} &U_1 = U_2 = 0,\ V_1 = V_2 = 0, \\ &T_1 = T_2,\ \ \frac{\partial T_1}{\partial Y} + \frac{\partial T_1}{\partial X} = \frac{\partial T_2}{\partial Y} + \frac{\partial T_2}{\partial X} \end{aligned}\right\} \text{on } Y = d^* \\ &U_2 = V_2 = 0, \qquad T_2 = T_f \quad \text{on } Y = d \end{aligned} \tag{1}$$

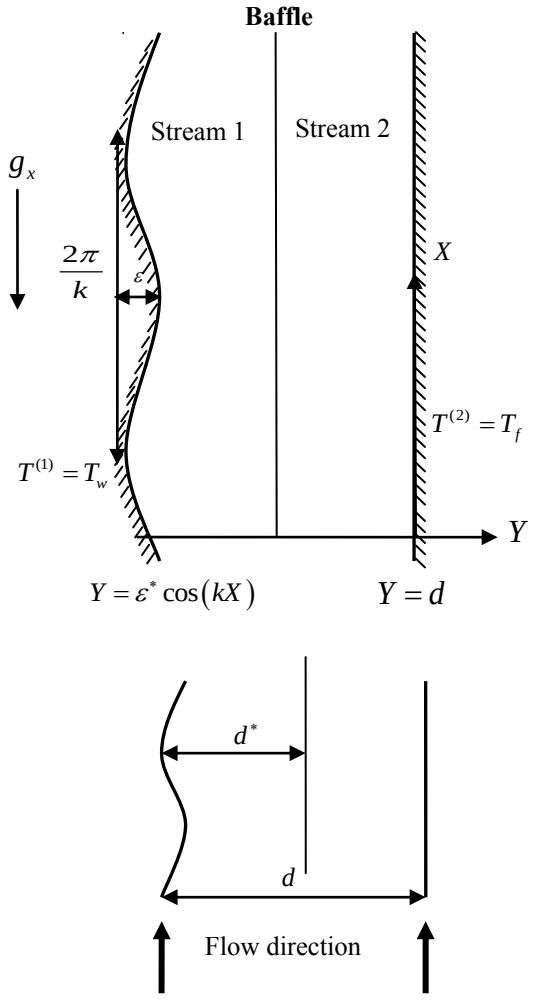

Fig. 1. Physical configuration of the double-passage channel

It is convenient to employ the following non-dimensional variables in the governing equations and boundary conditions for velocity and temperature:

$$x = \frac{X}{d},\ y = \frac{Y}{d},\ u_i = \frac{U_i d}{\nu},\ v_i = \frac{V_i d}{\nu},\ \theta = \frac{T - T_s}{T_w - T_s},\ \bar{p} = \frac{p^*}{\rho(\nu/d)^2} \tag{2}$$

where T_s is the fluid temperature in static condition. Doing this, one obtains the equation of continuity as

$$\frac{\partial u_i}{\partial x} + \frac{\partial v_i}{\partial y} = 0 \tag{3}$$

and the momentum equation becomes

$$\begin{aligned} &\rho\left(u_i \frac{\partial u_i}{\partial x} + v_i \frac{\partial u_i}{\partial y}\right) = -\frac{\partial \overline{P_i}}{\partial x} + \frac{\partial^2 u_i}{\partial x^2} + \frac{\partial^2 u_i}{\partial y^2} - K\left[2u_i \frac{\partial^3 u_i}{\partial x^3}\right. \\ &+2v_i \frac{\partial^3 u_i}{\partial x^2 \partial y} + u_i \frac{\partial^3 u_i}{\partial x \partial y^2} + u_i \frac{\partial^3 v_i}{\partial y \partial x^2} + v_i \frac{\partial^3 u_i}{\partial y^3} + v_i \frac{\partial^3 v_i}{\partial x \partial y^2} \\ &-6\frac{\partial u_i}{\partial x}\frac{\partial^2 u_i}{\partial x^2} + \frac{\partial u_i}{\partial y}\frac{\partial^2 v_i}{\partial x^2} - 4\frac{\partial u_i}{\partial y}\frac{\partial^2 u_i}{\partial x \partial y} - 2\frac{\partial v_i}{\partial x}\frac{\partial^2 v_i}{\partial y^2} - 3\frac{\partial v_i}{\partial x}\frac{\partial^2 u_i}{\partial x \partial y} \\ &\left.-\frac{\partial u_i}{\partial x}\frac{\partial^2 v_i}{\partial x \partial y} - 3\frac{\partial u_i}{\partial y}\frac{\partial^2 v_i}{\partial y^2} - \frac{\partial v_i}{\partial x}\frac{\partial^2 v_i}{\partial y^2} - \frac{\partial u_i}{\partial x}\frac{\partial^2 u_i}{\partial y^2}\right] - \rho\frac{g_x d^3}{\rho \nu^2} \end{aligned} \tag{4}$$

$$\rho\left(u_i\frac{\partial v_i}{\partial x}+v_i\frac{\partial v_i}{\partial y}\right)=-\frac{\partial \overline{P_i}}{\partial y}+\frac{\partial^2 v_i}{\partial x^2}+\frac{\partial^2 v_i}{\partial y^2}-K\Bigg[u_i\frac{\partial^3 u_i}{\partial x^2\partial y}$$
$$+u_i\frac{\partial^3 v_i}{\partial x^3}+v_i\frac{\partial^3 u_i}{\partial x\partial y^2}+v_i\frac{\partial^3 v_i}{\partial y\partial x^2}+2u_i\frac{\partial^3 v_i}{\partial x\partial y^2}+2v_i\frac{\partial^3 v_i}{\partial y^3}$$
$$-2\frac{\partial u_i}{\partial x}\frac{\partial^2 v_i}{\partial x^2}-2\frac{\partial v_i}{\partial x}\frac{\partial^2 v_i}{\partial y^2}-3\frac{\partial^2 u_i}{\partial x^2}\frac{\partial v_i}{\partial x}-3\frac{\partial v_i}{\partial y}\frac{\partial^2 u_i}{\partial x\partial y}$$
$$-3\frac{\partial u_i}{\partial y}\frac{\partial^2 v_i}{\partial x\partial y}-\frac{\partial v_i}{\partial y}\frac{\partial^2 v_i}{\partial x^2}-\frac{\partial u_i}{\partial y}\frac{\partial^2 u_i}{\partial x^2}-6\frac{\partial v_i}{\partial y}\frac{\partial^2 v_i}{\partial y^2}-4\frac{\partial v_i}{\partial x}\frac{\partial^2 v_i}{\partial x\partial y}\Bigg] \tag{5}$$

and the energy equation becomes

$$P\left(u_i\frac{\partial \theta_i}{\partial x}+v_i\frac{\partial \theta_i}{\partial y}\right)=\frac{\partial^2\theta_i}{\partial x^2}+\frac{\partial^2\theta_i}{\partial y^2} \tag{6}$$

and the dimensionless boundary conditions can be written as

$$u_1=v_1=0,\qquad \theta_1=1 \text{ on } y=\varepsilon\cos(\lambda x)$$
$$\left.\begin{aligned}&u_1=u_2=0,\ v_1=v_2=0,\\ &\theta_1=\theta_2,\ \frac{\partial\theta_1}{\partial y}+\frac{\partial\theta_1}{\partial x}=\frac{\partial\theta_2}{\partial y}+\frac{\partial\theta_2}{\partial x}\end{aligned}\right\}\ \text{on } Y=d^*$$
$$u_2=v_2=0,\qquad \theta_2=m \text{ on } Y=d \tag{7}$$

where

$P=\eta_0 c_p/k$, the Prandtl number

$\varepsilon=\varepsilon^*/d$, the dimensionless amplitude parameter

$\lambda=kd$, the dimensionless frequency parameter

$m=(T_1-T_s)/(T_w-T_s)$, the wall temperature ratio

$K=2K_0/(\rho d^2)$

and ρg_x is the buoyancy term in X-direction, where the subscript s denotes quantities in the static fluid condition.

Now, introducing the non-dimensional quantity as:

$G=d^3 g_x\beta(T_w-T_s)/\nu^2$

the Grashof number and using the equation of state, one has

$\rho=\rho_s\left(1-\beta(T-T_s)\right)$

η_0 is the limiting viscosity at small rate of shear which is given by

$$\eta_0=\int_0^\infty N(\tau)\,d\tau \text{ and } k_0=\int_0^\infty \tau N(\tau)\,d\tau$$

where $N(\tau)$ being the relaxation spectrum as introduced by Walters [24, 25]. This idealized model is a valid approximation of Walters fluid (model B') taking very short memories into account so that involving

$$\int_0^\infty \tau^n N(\tau)\,d\tau,\ n\geq 2$$

are neglected (Choudhury and Das [26]).

The conservation of mass considered at any cross section of the channel passage gives

$$\int_0^{y^*} u_1\,dy=y^*$$

and

$$\int_{y^*}^1 u_2\,dy=1-y^*$$

3. Solutions

Equations (4) to (6) are coupled non-linear partial differential equations and hence finding exact solutions is out of scope. However, for small values of the amplitude parameter ε, approximate solutions can be extracted through the perturbation method . The amplitude parameter ε is usually small and hence regular perturbation method can be strongly justified. Adopting this technique, solutions for velocity and temperature are assumed in the form

$$u_i(x,y)=u_{i0}(y)+\varepsilon u_{i1}(x,y)\quad v_i(x,y)=\varepsilon v_{i1}(x,y)$$
$$\bar{p}_i=p_{i0}(x)+\varepsilon p_{i1}(x,y),\ \theta_i(x,y)=\theta_{i0}(y)+\varepsilon\theta_{i1}(x,y) \tag{8}$$

where the perturbations u_{i1}, v_{i1}, p_{i1} and θ_{i1} are small compared with the mean or zeroth order quantities. Equations (3) to (7) yield the following non-dimensional equations.

Zeroth-order equations:

$$\frac{d^2u_{i0}}{dy^2}+G\theta_{i0}=0\quad \frac{d^2\theta_i}{dy^2}=0 \tag{9}$$

First order equations:

$$\frac{\partial u_{i1}}{\partial x}+\frac{\partial v_{i1}}{\partial y}=0 \tag{10}$$

$$u_{i0}\frac{\partial u_{i1}}{\partial x}+v_{i1}\frac{\partial u_{i0}}{\partial y}=-\frac{\partial\overline{P_{i1}}}{\partial x}+\frac{\partial^2 u_{i1}}{\partial x^2}+\frac{\partial^2 u_{i1}}{\partial y^2}-K\Bigg[2u_{i0}\frac{\partial^3 u_{i1}}{\partial x^3}$$
$$+u_{i0}\frac{\partial^3 u_{i1}}{\partial x\partial y^2}+u_{i0}\frac{\partial^3 v_{i1}}{\partial y\partial x^2}+v_{i1}\frac{\partial^3 u_{i0}}{\partial y^3}+\frac{\partial u_{i0}}{\partial y}\frac{\partial^2 v_{11}}{\partial x^2}-4\frac{\partial u_{i0}}{\partial y}\frac{\partial^2 u_{i1}}{\partial x\partial y}$$
$$-2\frac{\partial v_{i1}}{\partial y}\frac{\partial^2 u_{i0}}{\partial y^2}-3\frac{\partial u_{i0}}{\partial y}\frac{\partial^2 v_{i1}}{\partial y^2}-\frac{\partial u_{i1}}{\partial x}\frac{\partial^2 u_{i0}}{\partial y^2}\Bigg]-G\theta_1 \tag{11}$$

$$u_{i0}\frac{\partial v_{i1}}{\partial x}=-\frac{\partial\overline{P_{i1}}}{\partial y}+\frac{\partial^2 v_{i1}}{\partial x^2}+\frac{\partial^2 v_{i1}}{\partial y^2}-K\Bigg[u_{i0}\frac{\partial^3 u_{i1}}{\partial x^2\partial y}+2u_{i0}\frac{\partial^3 v_{i1}}{\partial x\partial y^2}$$
$$+u_{i0}\frac{\partial^3 v_{i1}}{\partial x^3}-2\frac{\partial v_{i1}}{\partial x}\frac{\partial^2 u_{i0}}{\partial x^2}-3\frac{\partial u_{i0}}{\partial y}\frac{\partial^2 v_{i1}}{\partial x\partial y}-\frac{\partial u_{i0}}{\partial y}\frac{\partial^2 u_{i1}}{\partial x^2}\Bigg] \tag{12}$$

$$P\left(u_{i0}\frac{\partial\theta_{i1}}{\partial x}+v_{i1}\frac{d\theta_{i0}}{dy}\right)=\frac{\partial^2\theta_{i1}}{\partial x^2}+\frac{\partial^2\theta_{i1}}{\partial y^2} \tag{13}$$

In deriving Eqn. (9), the constant pressure gradient term $\frac{\partial}{\partial x}(p_0-p_s)$ has been taken equal to zero following (Ostrach [27]). In view of Eqn. (8) the boundary condition in Eqn. (7) can be split up into the following two parts.

Zeroth-order boundary conditions:

$$u_{10}=0,\qquad \theta_{10}=1 \text{ on } y=0$$
$$u_{10}=u_{20}=0,\ \theta_{10}=\theta_{20},\ \frac{d\theta_{10}}{dy}=\frac{d\theta_{20}}{dy} \text{ on } y=y^*$$
$$u_{20}=0,\ \theta_{20}=m \text{ on } \qquad y=1 \tag{14}$$

First-order boundary conditions:

$$u_{11} = -rp\left(e^{i\lambda x}\frac{du_{10}}{dy}\right), \qquad v_{11} = 0, \ \text{on } y = 0$$

$$\theta_{11} = -rp\left(e^{i\lambda x}\frac{d\theta_{10}}{dy}\right)\text{on} \quad y = 0 \tag{15}$$

$$u_{11} = u_{21}=0, \ v_{11} = v_{21}=0, \ \theta_{11} = \theta_{21}, \text{ on } y = y^*$$

$$u_{21} = 0, \ v_{21} = 0, \ \theta_{21} = 0, \ \text{on} \qquad y = 1$$

where rp represents the real part

The solutions for zeroth-order velocity u_{i0} and zeroth-order temperature θ_{i0} satisfying the differential equation (9) and the boundary conditions (14) are given by

Stream 1:

$$\theta_{10} = c_1 y + c_2 \tag{16}$$

$$u_{10} = l_1 y^3 + l_2 y^2 + d_1 y + d_2 \tag{17}$$

Stream 2:

$$\theta_{20} = c_7 y + c_8 \tag{18}$$

$$u_{20} = l_6 y^3 + l_7 y^2 + d_{11} y + d_{12} \tag{19}$$

In order to solve Eqs. (10) to (13) for the first-order quantities, it is convenient to introduce stream function $\bar{\psi}$ in the following form:

$$u_{i1} = -\frac{\partial \bar{\psi}_{i1}}{\partial y}, \ v_{i1} = \frac{\partial \bar{\psi}_{i1}}{\partial x} \ \text{ for } i = 1,2 \tag{20}$$

The stream function approach reduces the number of dependent variables to be solved and also eliminates pressure from the list of variables. Differentiating Eqn. (11) with respect to y and differentiating Eqn. (12) with respect to x and then subtracting Eqn. (11) with Eqn. (12) results in the elimination of pressure p_{i1}. Assuming the stream function and temperature as $\bar{\psi}_{i1}(x,y) = e^{i\lambda x}\psi_{i1}(y)$, $\theta_{i1}(x,y) = e^{i\lambda x}t_{i1}(y)$ and using them in Eqs. (10) to (13) after elimination of p_{i1}, causes these equations to be expressed in terms of the stream function ψ and t in the forms

$$\psi_i^{iv} - \psi_i^{"}\left(2\lambda^2 + i\lambda u_{i0}\right) + \psi_i\left(\lambda^4 + i\lambda u_{i0}^{"} + iu_{i0}\lambda^3\right) + K\,\mathrm{i}(2u_{i0}\lambda^3\psi_i^{"} - \lambda u_{i0}\psi_i^{iv} - 2u_{i0}^{'}\lambda^3\psi_i^{'} - 3u_{i0}^{"}\lambda^3\psi_1 + \lambda u_{10}^{iv}\psi_1 - \lambda^5 u_{10}\psi_i) = Gt_i^{'} \tag{21}$$

$$t_i^{"} - \lambda^2 t_i = P\,\mathrm{i}\,\lambda\left(u_{10}t_i + \psi_i\theta_{i0}^{'}\right) \tag{22}$$

where i is the coefficient of imaginary part and suffix i=1,2 denotes stream-1 and stream-2 respectively.

The boundary and interface conditions as defined in Eq. (15) can be written in terms of ψ and t as

$$\begin{aligned}
&\psi_1^{'} = u_{10}^{'}, \psi_1 = 0, \ \ t_1 = -\theta_{10}^{'} \text{ on} \qquad y = 0\\
&\psi_1^{'} = 0, \ \ \psi_1 = 0, \ \ \psi_2^{'} = 0, \ \ \psi_2 = 0, \ \ \text{on } y = y^*\\
&t_1 = t_2, \ \ t_1^{'} = t_2^{'}, \ \ \text{on } y = y^*\\
&\psi_2^{'} = 0, \ \ \psi_2 = 0, \ \ t_2 = 0, \ \ \text{on} \qquad y = 1
\end{aligned} \tag{23}$$

We restrict our attention to the real parts of the solutions for the perturbed quantities ψ, t, u_{i1} and v_{i1}.

Consider only small values of λ on substituting

$$\psi(\lambda, y) = \sum_{r=0}^{\infty}\lambda^r\psi_r, \qquad t(\lambda, y) = \sum_{r=0}^{\infty}\lambda^r t_r \tag{24}$$

into Eqs. (21) to (23) we obtain to the order of λ, the following set of ordinary differential equations

Zeroth order

$$t_{i0}^{"} = 0 \tag{25}$$

$$\psi_{i0}^{iv} = Gt_{i0}^{'} \tag{26}$$

First order

$$t_{i1}^{"} = P\,\mathrm{i}\left(u_{i0}t_{i0} + \psi_{i0}\theta_{10}^{'}\right) \tag{27}$$

$$\psi_{i1}^{iv} = iu_{i0}\psi_{i0}^{"} - iu_{i0}^{"}\psi_{i0} + \mathrm{i}\,K\left(u_{i0}\psi_{i0}^{iv} - u_{i0}^{iv}\psi_{10}\right) + Gt_{i1}^{'} \tag{28}$$

The zeroth-order boundary and interface conditions in terms of stream function and temperature are

$$\begin{aligned}
&\psi_{10}^{'} = u_{10}^{'}, \qquad \psi_{10} = 0, \ t_{10} = -\theta_{10}^{'} \qquad \text{on } y = 0\\
&\psi_{10}^{'} = 0, \ \psi_{10} = 0, \ \psi_{20}^{'} = 0, \ \psi_{20} = 0, \text{ on} \qquad y = y^*\\
&t_{10} = t_{20}, \ t_{10}^{'} = t_{20}^{'}, \text{ on} \qquad y = y^*\\
&\psi_{20}^{'} = 0, \ \psi_{20} = 0, \ t_{20} = 0, \ \ \text{on} \qquad y = 1
\end{aligned} \tag{29}$$

The first-order boundary and interface conditions in terms of stream function and temperature are

$$\begin{aligned}
&\psi_{11}^{'} = 0, \ \psi_{11} = 0, \ t_{11} = 0 \quad \text{on} \qquad y = 0\\
&\psi_{11}^{'} = 0, \ \psi_{11} = 0, \ \psi_{21}^{'} = 0, \ \psi_{21} = 0, \text{ on } y = y^*\\
&t_{11} = t_{21}, \ t_{11}^{'} = t_{21}^{'}, \ \text{on } y = y^*\\
&\psi_{21}^{'} = 0, \ \psi_{21} = 0, \ t_{21} = 0, \ \ \text{on} \qquad y = 1
\end{aligned} \tag{30}$$

The set of Eqs. (25) to (28) subject to the boundary and interface conditions [Eqs. (29) and (30)] have been solved exactly for ψ and t. From these solutions, the first-order quantities can be put in the form,

$$\psi = \left(\psi_{rp} + \mathrm{i}\,\psi_{\mathrm{i}\,p}\right) = \psi_{i0} + \lambda\psi_{i1}, \ t = \left(t_{rp} + \mathrm{i}\,t_{\mathrm{i}\,p}\right)_j = t_{i0} + \lambda t_{i1} \tag{31}$$

where the suffix rp denotes the real part and $\mathrm{i}\,p$ denotes the imaginary part. Considering only the real part, the expression for the first-order velocity and temperature become

$$u_{i1} = -\cos(\lambda x)\psi_{i0}^{'} + \lambda\psi_{i1}^{'}\sin(\lambda x) \tag{32}$$

$$v_{i1} = -\lambda^2\cos(\lambda x)\psi_{i1} - \lambda\psi_{i0}\sin(\lambda x) \tag{33}$$

$$\theta_{i1} = \cos(\lambda x)(t_{i0}) - \lambda t_{i1}\sin(\lambda x) \tag{34}$$

The first-order and total solutions are not given due to space limitations.

3.1. Skin friction and Nusselt number:

The shearing stress σ_{xy} at any point in the fluid in non-dimensional form is given by

$$\sigma_{xy} = \frac{d^2\bar{\sigma}_{xy}}{\rho\nu^2} = u_0^{'}(y) + \varepsilon e^{i\lambda x}\bar{u}_1^{'}(y) + \mathrm{i}\,\varepsilon\lambda e^{i\lambda x}\bar{v}_1(y) + K\varepsilon\begin{pmatrix} 3u_0^{'}e^{i\lambda x}\bar{v}_1^{'}(y) + u_0^{'}(\mathrm{i}\,\lambda)e^{i\lambda x}\bar{u}_1(y) \\ -u_0^{"}(y)e^{i\lambda x}\bar{v}_1(y) + u_0(y)\lambda^2 e^{i\lambda x}\bar{v}_1(y) \\ u_0(y)(\mathrm{i}\,\lambda)e^{i\lambda x}\bar{u}_1^{'}(y) \end{pmatrix} \tag{35}$$

At the wavy wall, $y=\varepsilon\cos(\lambda x)$, the skin friction takes the form

$$\sigma_w=\sigma_0^0(0)+\varepsilon(u_{01}^{''}\cos(\lambda x)+\lambda\psi_{11}^{''}(0)\sin(\lambda x) -\psi_{10}^{''}(0)\cos(\lambda x))-2\lambda\varepsilon K\sigma_0^0(0)(\psi_{11}^{'}(0)\sin(\lambda x) +\lambda\psi_{11}^{'}(0)\cos(\lambda x)) \quad (36)$$

and at the flat wall, $y=1$, the skin friction takes the form

$$\sigma_f=\sigma_1^0(0)+\varepsilon\left(-\psi_{20}^{''}(0)\cos(\lambda x)+\lambda\psi_{21}^{''}(0)\sin(\lambda x)\right) \varepsilon\lambda K\begin{pmatrix}\lambda u_{20}^{''}(1)\psi_{21}(1)\cos(\lambda x)\\ -2u_{20}^{'}(1)\left(\psi_{21}^{'}(1)\sin(\lambda x)+\lambda\psi_{21}^{'}\cos(\lambda x)\right)\end{pmatrix} \quad (37)$$

where $\sigma_0^0=u_{10}^{'}(0)$ and $\sigma_1^0=u_{20}^{'}(1)$ are the zeroth-order skin-friction at the walls, and $\bar{u}_1(y)$ and $\bar{v}_1(y)$ are given by $u(x,y)=e^{i\lambda x}\bar{u}_1(y)$, $v_1(x,y)=e^{i\lambda x}\bar{v}_1(y)$

The non-dimensional heat transfer coefficient known as Nusselt number (Nu) is given by

The dimensionless Nusselt number is given by

$$Nu=\frac{\partial\theta}{\partial y}=\theta_0^{'}(y)+\varepsilon\,\mathrm{Re}\left(e^{i\lambda x}\theta_1^{'}(y)\right) \quad (35)$$

At the wavy wall $y=-1+\varepsilon\cos(\lambda x)$ Nusselt number Nu_w takes the form

$$Nu_w=Nu_0^0+\varepsilon\begin{pmatrix}\theta_{10}^{'}(0)\cos(\lambda x)+t_{10}^{'}(0)\cos(\lambda x)\\ -\lambda t_{11}^{'}(0)\sin(\lambda x)\end{pmatrix}, \quad (36)$$

and at the flat wall $y=1$,

$$Nu_f=Nu_1^0+\varepsilon\left(t_{20}^{'}(1)\cos(\lambda x)-\lambda t_{21}^{'}(1)\sin(\lambda x)\right) \quad (37)$$

where

$$Nu_0^0=\left(\frac{d\theta_{10}}{dy}\right)_{y=-1} \qquad Nu_1^0=\left(\frac{d\theta_{20}}{dy}\right)_{y=1}$$

The velocity and temperature solutions are numerically evaluated for several sets of values of the governing parameters. Also, the wall skin frictions σ_w, σ_f and the wall Nusselt numbers Nu_w, Nu_f are calculated numerically and some of the qualitative interesting features are presented.

4. Result and Discussion

Free convective flow and heat transfer of Walter's fluid (model *B'*) in a vertical channel one of whose walls is wavy, containing a thin conducting baffle is studied analytically. The non-linear partial differential equations governing the motion have been solved by a linearization technique wherein the flow is assumed to be of two parts; a mean part and a perturbed part. Exact solutions are obtained for the mean part and the perturbed pert is solved using long wavy approximation. The Prandtl number, wave number, and amplitude are fixed as 0.7, 0.01, and 0.1, respectively for the computation, whereas the Grashof number, wall temperature ratio, viscoelastic parameter and λx are fixed as 20, -1, 0, and 1.57079632, respectively for all the graphs except the varying one.

The effect of the Grashof number G on the main and cross velocity is shown in Figs. 2a,b,c at three different baffle positions $(y^*=0.2,\ 0.5 \text{ and } 0.8)$. As the Grashof number increases, the main velocity u increases near the left (hot) wall and decreases at the right (cold) wall. The larger the value of G, the stronger the upward velocity. Especially, for sufficient large values of G, a flow reversal phenomenon is predicted near the right (cold) wall as shown in Fig. 2a, which can also be observed for Newtonian single passage flow examined by Aung and Warku [28]. For each graph the maximum point of the main velocity moves to the left (hotter) wall for increasing values of G and thus, the velocity decreases near the right (colder) wall.

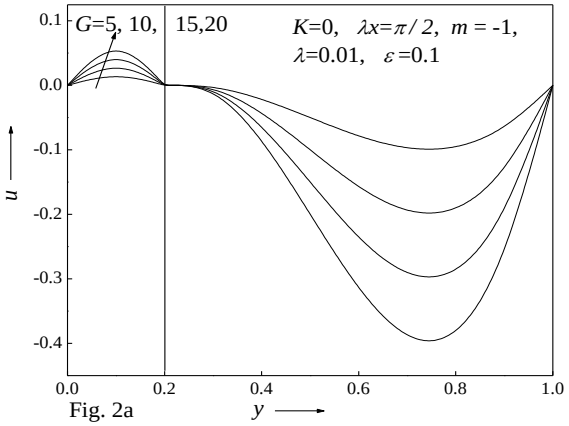

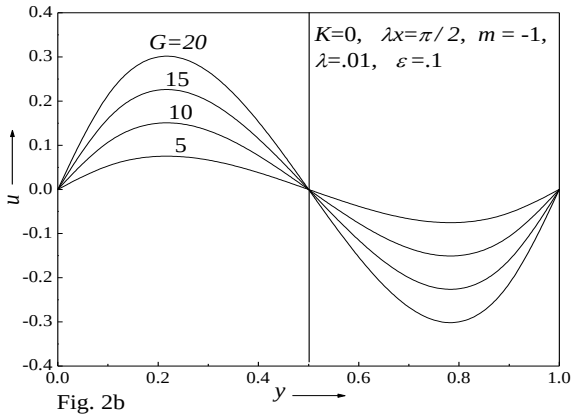

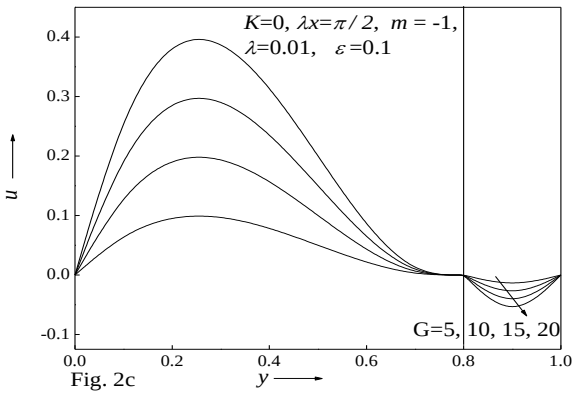

Fig. 2 Main velocity profiles for different values of Grashof number G

The effect of G on the cross velocity is exactly opposite to the effect of G on the main velocity as seen in Figs. 3a,b,c. That is, as G increases, the cross velocity v decreases near the left (hot) wall and increases at the right (cold) wall. Also, as G increases, the maximum point of the cross velocity moves to the right (colder) wall and thus, the cross velocity decreases at the left (hot) wall.

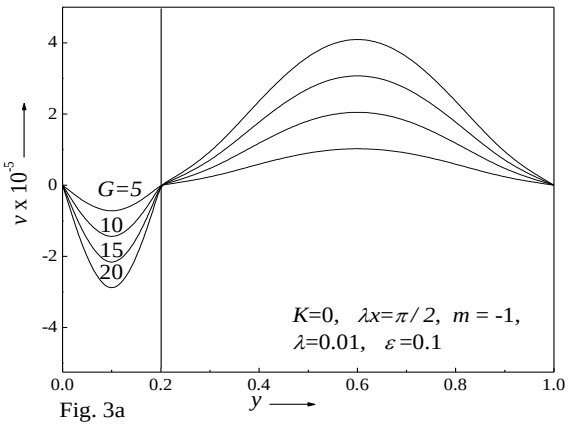

Fig. 3a

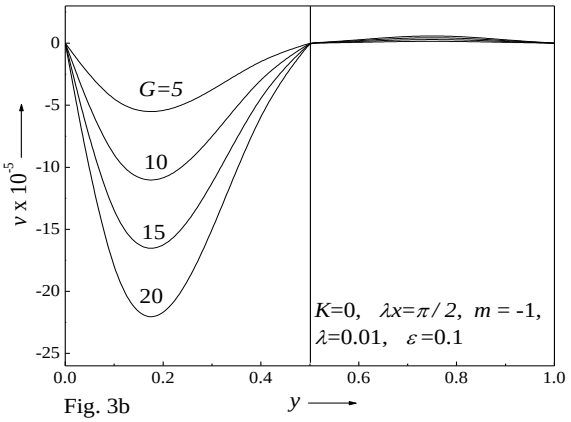

Fig. 3b

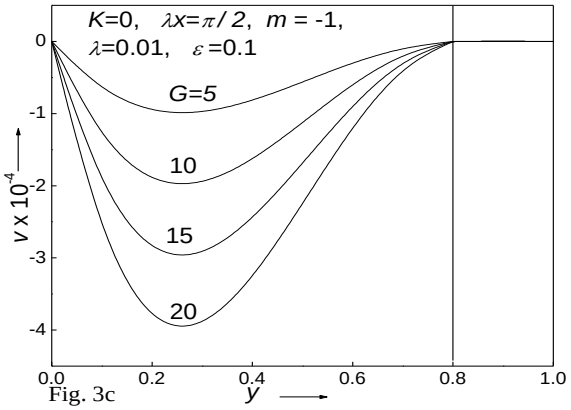

Fig. 3c

Fig.3 Cross velocity profiles for differnt values of Grashof number G

The effect of the Grashof number G on the temperature is shown in Table 1. It is noticed that the temperature remains almost invariant at all baffle positions for G=10 and G=200.

Table 1. Temperature values for different Grashof number and baffle position.

y	$y^* = 0.2$		y	$y^* = 0.5$	
	G=10	G=200		G=10	G=200
0	1.0	1.00000	0	1.0	1.00000
0.1	0.8	0.79999	0.1	0.8	0.80000
0.2	0.6	0.59997	0.2	0.6	0.60000
0.2	0.6	0.59997	0.3	0.4	0.40000
0.3	0.4	0.39996	0.4	0.2	0.19999
0.4	0.2	0.19994	0.5	0.0	0.0
0.5	0.0	0.0000	0.5	0.0	0.0
0.6	-0.2	-0.20008	0.6	-0.2	-0.20003
0.7	-0.4	-0.40007	0.7	-0.4	-0.40004
0.8	-0.6	-0.60005	0.8	-0.6	-0.60003
0.9	-0.8	-0.80003	0.9	-0.8	-0.80002
1.0	-1.0	-1.00000	1.0	-1.0	-1.00000

y	$y^* = 0.8$	
	$G = 10$	$G = 200$
0	1.00000	1.00000
0.1	0.80000	0.79995
0.2	0.60000	0.59990
0.3	0.39999	0.39987
0.4	0.19999	0.19985
0.5	-7.50E-6	-1.5E-4
0.6	-0.20001	-0.20013
0.7	-0.40001	-0.40010
0.8	-0.60000	-0.60007
0.8	-0.60000	-0.60007
0.9	-0.80000	-0.80004
1.0	-1.00000	-1.00000

Figures 4a,b,c show the effect of the wall temperature ratio m on the main velocity ($m = -1$ means that the average of the temperatures of the two walls is equal to that of the static temperature, $m = 0$ corresponds to the case that the temperature of the flat wall is equal to the static temperature, $m = 1$ means that the wavy and flat wall are maintained at equal temperature and $m > 1$ implies that the wall temperatures are unequal). As m increases, the main velocity u increases in both streams at the baffle positions 0.2, 0.5 and 0.8. and the flow reversal is observed in stream 2 for $m = -1$. It is also observed that the main velocity profile for $m = 0$ lies in between $m = -1$ (below) and 1 (above). When the baffle position is near the left wall, the variations of m are not very effective on the main velocity but its effect is dominant when the baffle position moves to the center and near to the right wall as seen in Fig. 4.

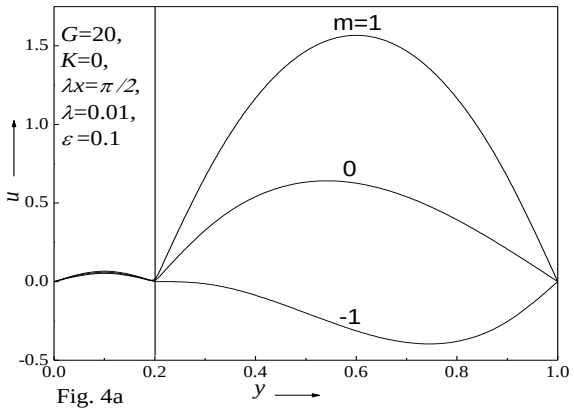

Fig. 4a

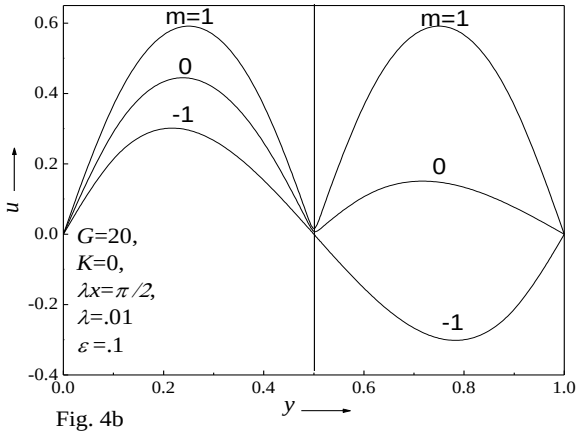

Fig. 4b

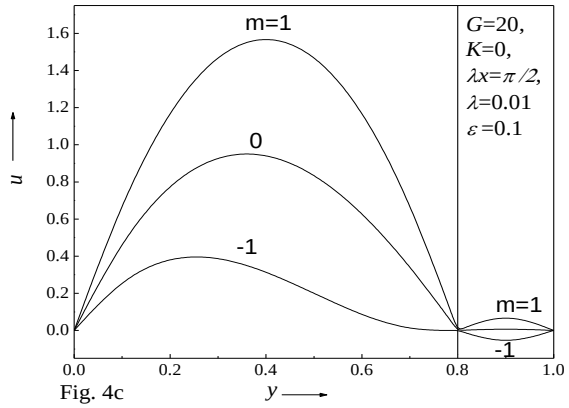

Fig. 4c

Fig. 4 Main velocity profiles for different values of wall temperature ratio m

The effect of m on the cross velocity is opposite to its effect on the main velocity. That is, as m increases the cross velocity decreases at all baffle positions as seen in Figs. 5a,b,c. The velocity profile for $m=0$ lies in between $m=1$ (below) and -1 (above). The effect of m on the cross velocity is not effective for the baffle position at the right wall when compared to the baffle position at the left and at the center of the channel.

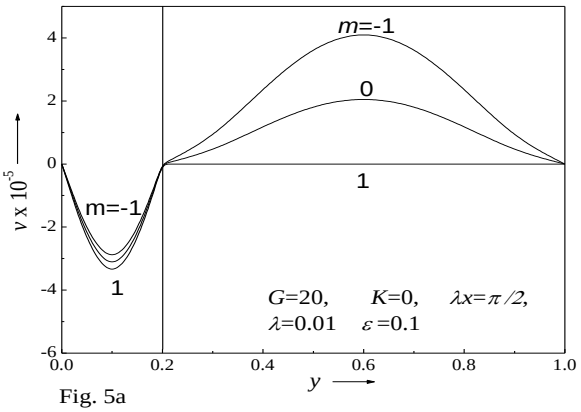

Fig. 5a

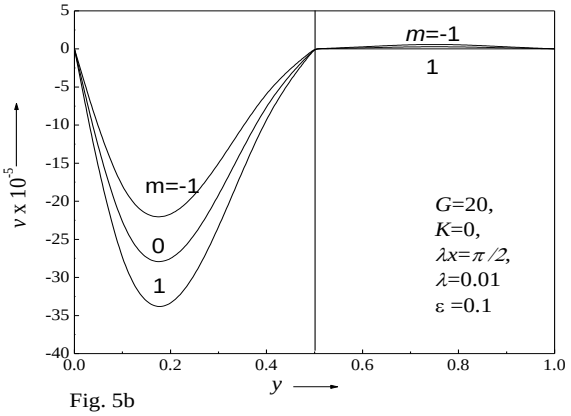

Fig. 5b

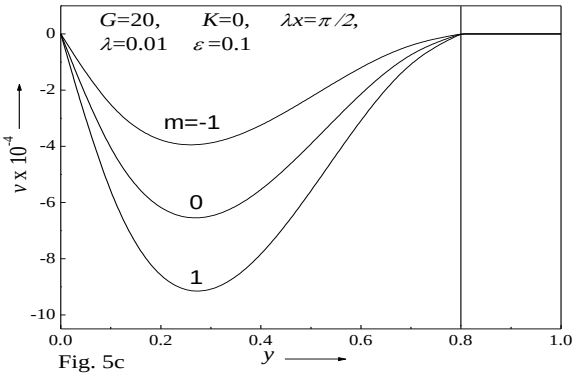

Fig. 5c

Fig. 5 Cross velocity for different values of wall temerature ratio m

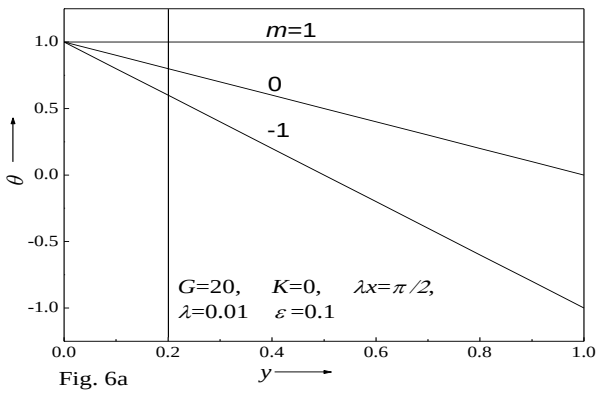

Fig. 6a

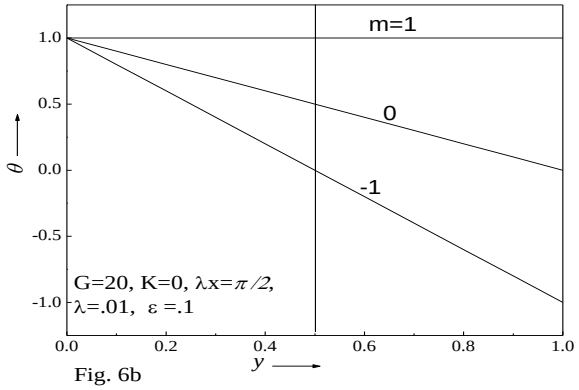

Fig. 6b

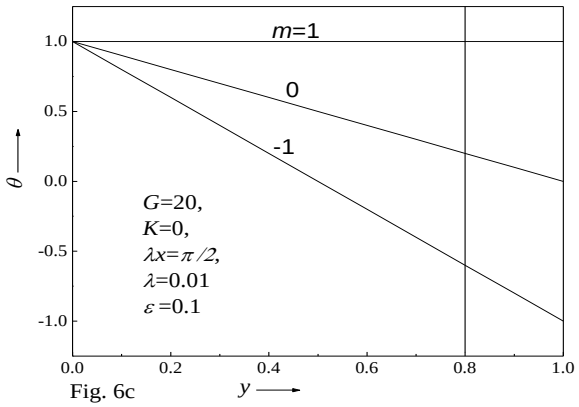

Fig. 6c

Fig. 6 Temperature profiles for different values of wall temperature ratio m

The effect of the wall temperature ratio m on the temperature field is shown in Figs. 6a,b,c. As m increases, the temperature increases at all baffle positions and the magnitude of promotion remains the same for $y^* = 0.2$, 0.5 and 0.8.

The effects of the viscoelastic parameter K on the main and cross velocities and temperature are shown in Tables 2a, 2b and 2c, respectively. As K increases, the main velocity remains constant up to the order of 10^{-4} and decreases from 10^{-5} and onwards at all baffle positions. However, there is no effect of the viscoelastic parameter K on the cross velocity (Table 2b) and on temperature (Table 2c).

Table 2a Main velocity for different viscoelastic parameter and baffle position

y	$y^* = 0.2$		
	$K = 0.0$	$K = 0.15$	$K = 0.3$
0	0	0	0
0.1	0.080000	0.080000	0.080000
0.2	-5.55099E-17	-5.5509E-17	-5.551E-17
0.2	3.88402E-16	3.88937E-16	3.88861E-16
0.3	1.853419E-5	2.347586E-5	2.841753E-5
0.4	-0.079974	-0.079968	-0.079961
0.5	-0.199978	-0.199973	-0.199968
0.6	-0.319991	-0.319990	-0.319989
0.7	-0.400010	-0.400013	-0.400017
0.8	-0.400029	-0.400036	-0.400043
0.9	-0.280034	-0.280040	-0.280047
1.0	8.88206E-16	8.88206E-16	8.8865E-16
y	$y^* = 0.5$		
	$K = 0.0$	$K = 0.15$	$K = 0.3$
0	0	0	0
0.1	0.239962	0.239961	0.239959
0.2	0.319972	0.319971	0.319970
0.2	0.280013	0.280014	0.280015
0.3	0.160047	0.160049	0.160051
0.4	-1.10991E-16	-1.11005E-16	-1.10998E-16
0.5	-1.11466E-16	-1.11067E-16	-1.1123E-16
0.6	-0.159986	-0.159985	-0.159983
0.7	-0.279990	-0.279989	-0.279989
0.8	-0.320005	-0.320006	-0.320007
0.9	-0.240017	-0.240018	-0.240020
1.0	8.87984E-16	8.87984E-16	8.88428E-16
y	$y^* = 0.8$		
	$K = 0.0$	$K = 0.15$	$K = 0.3$
0	0	0	0
0.1	0.279807	0.279800	0.279794
0.2	0.399739	0.399732	0.399725
0.2	0.399790	0.399786	0.399782
0.3	0.319934	0.319935	0.319936
0.4	0.200125	0.200130	0.200135
0.5	0.080286	0.080292	0.080299
0.6	2.979709E-4	3.029126E-4	3.078542E-4
0.7	-8.87644E-16	-8.87311E-16	-8.877E-16
0.8	7.14706E-19	-3.1225E-19	6.8695E-19
0.9	-0.080000	-0.080000	-0.080000
1.0	8.88428E-16	8.88206E-16	8.88428E-16

Table 2b. Cross velocity values for different viscoelastic parameter and baffle position.

y	$y^* = 0.2$	y	$y^* = 0.5$
	K=0.0,0.15,0.3		K=0.0,0.15,0.3
0	0	0	0
0.1	-4.316667E-5	0.1	-2.106667E-4
0.2	1.27935E-19	0.2	-2.34E-4
0.2	8.84275E-19	0.3	-1.54E-4
0.3	8.166667E-6	0.4	-5.066667E-5
0.4	2.4E-5	0.5	1.52655E-19
0.5	3.75E-5	0.5	-8.46545E-19
0.6	4.266667E-5	0.6	2.666667E-6
0.7	3.75E-5	0.7	6E-6
0.8	2.4E-5	0.8	6E-6
0.9	8.166667E-6	0.9	2.666667E-6
1.0	-2.22044E-19	1	-2.22044E-19
y	$y^* = 0.8$		
	K=0.0,0.15,0.3		
0	0		
0.1	-2.776667E-4		
0.2	-3.96E-4		
0.3	-4E-4		
0.4	-3.306667E-4		
0.5	-2.25E-4		
0.6	-1.16E-4		
0.7	-3.266667E-5		
0.8	1.66533E-18		
0.8	7.77156E-19		
0.9	1.666667E-7		
1	-2.22044E-19		

Table 2c. Temperature values for different viscoelastic parameter and baffle position.

y	$y^* = 0.2$	y	$y^* = 0.5$
	$K = 0.0, 0.15, 0.3$		$K = 0.0, 0.15, 0.3$
0	1	0	1
0.1	0.8	0.1	0.8
0.2	0.6	0.2	0.6
0.2	0.6	0.3	0.4
0.3	0.4	0.4	0.2
0.4	0.19999	0.5	-1.82224E-6
0.5	-7.28049E-6	0.5	-1.82224E-6
0.6	-0.20001	0.6	-0.2
0.7	-0.40001	0.7	-0.4
0.8	-0.60001	0.8	-0.6
0.9	-0.8	0.9	-0.8
1	-1	1	-1

y	$y^* = 0.8$
	$K = 0.0, 0.15, 0.3$
0	1
0.1	0.8
0.2	0.59999
0.3	0.39999
0.4	0.19998
0.5	-1.50067E-5
0.6	-0.20001
0.7	-0.40001
0.8	-0.60001
0.8	-0.60001
0.9	-0.8
1	-1

The effect of λx on the main velocity are shown in Figs. 7a,b,c. As λx increases, the main velocity increases near the wavy wall and reverses its direction near the baffle position and remains constant at the flat wall at all baffle positions.

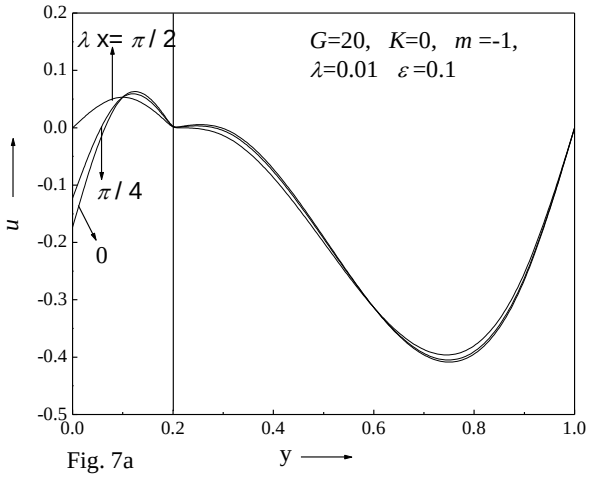

Fig. 7a

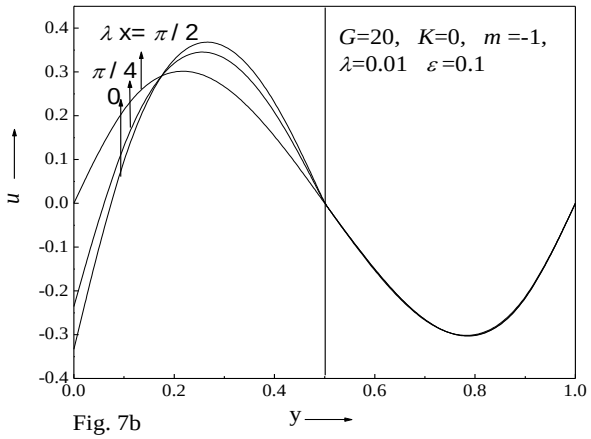

Fig. 7b

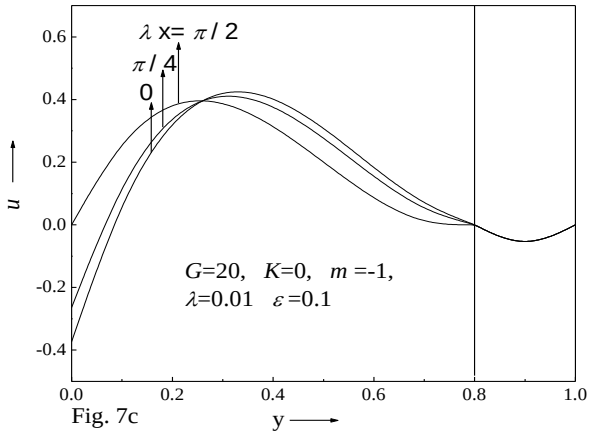

Fig. 7c

Fig. 7 Main velocity profiles for different values of λ x

The effect of λx on the cross velocity is shown in Figs. 8a,b,c. As λx increases, the cross velocity decreases in stream 1 and increases in stream 2 for the baffle positions at the left, center and the right walls. However, there is no effect of λx at the right wall when $y^* = 0.8$.

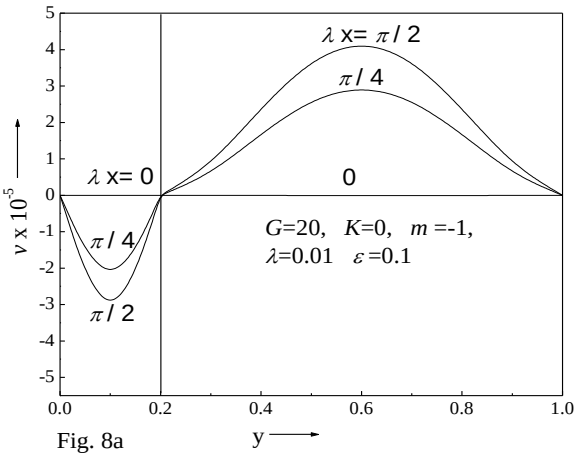

Fig. 8a

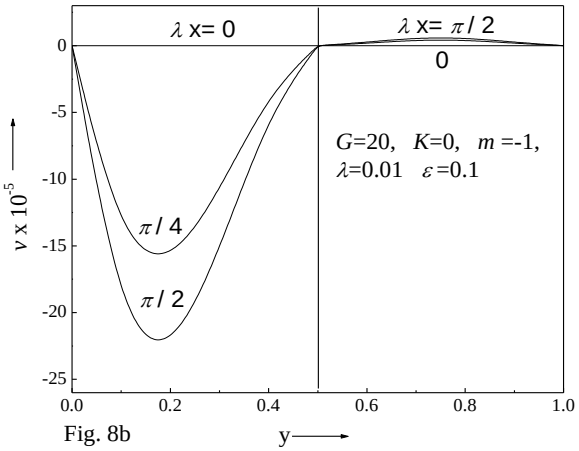

Fig. 8b

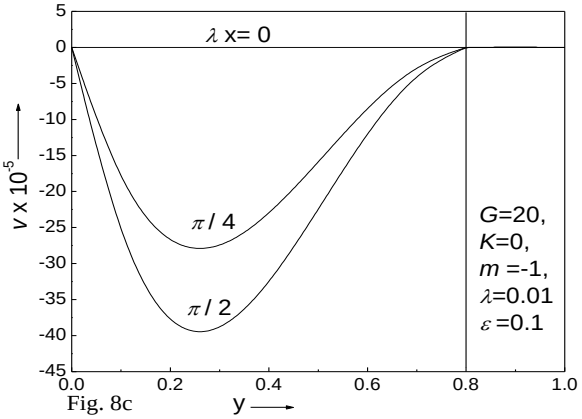

Fig. 8c

Fig. 8 Cross velocity profiles for different values of λ x

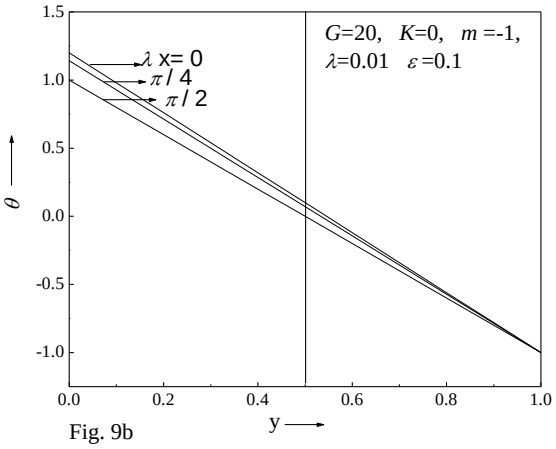

Fig. 9b

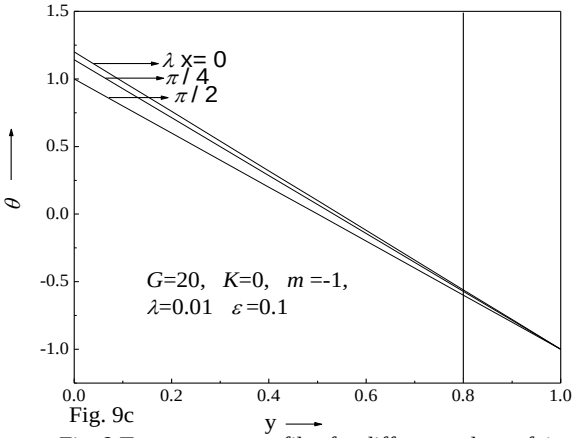

Fig. 9c

Fig. 9 Temperature profiles for different values of λ x

The effect of λx on the temperature is presented in Figs. 9a,b,c. It is seen that increasing λx causes the temperature to decrease at the wavy wall while it remains unchanged at the flat wall for the baffle positions near the left, center and right walls. The magnitude of suppression remains the same at any position of the baffle.

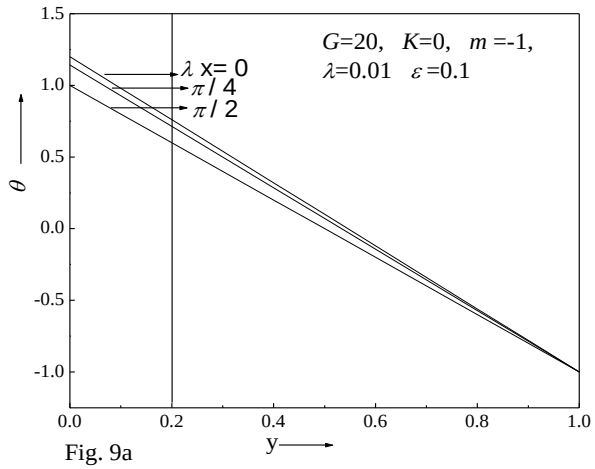

Fig. 9a

The values of the skin friction and the Nusselt numbers for different physical parameters are shown in Tables 3a and 3b, respectively for the values of $G = 20, K = 0.3, m = -1,$ $\lambda = 0.01, \varepsilon = 0.1$ except the varying parameter.

The effects of the Grashof number and wall temperature ratio are seen to increase the skin friction at the wavy wall and decrease at the flat wall at all baffle positions. The effects of the viscoelastic parameter, wave number and the amplitude parameter are predicted to decrease the skin friction at the wavy wall while it remains constant at the flat wall as seen in Table 3a.

Table 3a. Skin friction at the wavy and flat wall

	σ_w		
G	$y^* = 0.2$	$y^* = 0.5$	$y^* = 0.8$
20	1.99757	4.98372	7.95321
100	9.93918	24.593	38.8303
200	19.7567	48.372	75.3213
m			
-1	1.7315	3.32597	3.7222
0	1.86454	4.15527	5.84065
1	1.99757	4.98372	7.95321
K			
0	1.99997	4.99872	7.99161
0.15	1.99877	4.99122	7.97241
0.3	1.99757	4.98372	7.95321

λ			
0	2	5	8
0.1	1.97567	4.8372	7.53213
0.5	1.87836	4.18601	5.66065
ε			
0	2	5	8
0.1	1.99757	4.98372	7.95321
0.5	1.98784	4.9186	7.76606
	σ_f		
	$y^* = 0.2$	$y^* = 0.5$	$y^* = 0.8$
G			
20	-8	-5	-2
100	-40	-25	-10
200	-80	-50	-20
m			
-1	3.73419	3.33384	1.73346
0	-2.13329	-0.83323	-0.1333
1	-8	-5	-2
K			
0	-8	-5	-2
0.15	-8	-5	-2
0.3	-8	-5	-2
λ			
0	-8	-5	-2
0.1	-8	-5	-2
0.5	-8	-5	-2
ε			
0	-8	-5	-2
0.1	-8	-5	-2
0.5	-8	-5	-2

In addition, the effect of the Grashof number is found to increase the rate of heat transfer at the wavy wall and decrease at the flat wall at all baffle positions. The effect of the wall temperature ratio is seen to increase the heat transfer at both walls at all baffle positions. The effect of the wave number is found to decrease the rate of heat transfer at the wavy wall and increase at the flat wall for $G = 500$. The effect of the amplitude parameter ε is predicted to decrease the heat transfer at both walls as seen Table 3b.

Table 3b. Nusselt number at the wavy and flat wall

	Nu_w		
G	$y^* = 0.2$	$y^* = 0.5$	$y^* = 0.8$
20	-0.99994	-0.99998	-1
100	-0.99972	-0.99991	-0.99999
200	-0.99944	-0.99981	-0.99997
m			
-1	-2.00001	-2	-2.00005
0	-0.99994	-0.99998	-1
1	0	0	0
λ			
0	-2.14142	-2.14142	-2.14142
0.1	-2.14328	-2.14099	-2.15029
1	-2.16005	-2.13712	-2.23014
ε			
0	-2	-2	-2
0.1	-2.14161	-2.14138	-2.14231
0.5	-3.41608	-3.41378	-3.42309
	Nu_f		
G	$y^* = 0.2$	$y^* = 0.5$	$y^* = 0.8$
20	-1.00006	-1.00001	-1.00001
100	-1.00028	-1.00007	-1.00003
200	-1.00055	-1.00014	-1.00006
m			
-1	-1.99997	-1.99998	-1.99996
0	-1.00006	-1.00001	-1.00001
1	0	0	0
λ			
0	-2.14142	-2.14142	-2.14142
0.1	-2.13636	-2.13841	-2.13511
1	-2.09076	-2.11134	-2.07835
ε			
0	-2	-2	-2
0.1	-2.14091	-2.14112	-2.14079
0.5	-3.40915	-3.41121	-3.40791

5. CONCLUSION

The characteristics of flow and heat transfer of viscoelastic (Walters fluid Model B') fluid in a vertical channel whose one of its walls is wavy in a double-passage channel with a perfectly conducting baffle are investigated. According to the results, the following conclusions can be drawn:

1. The maxima of the main velocity profiles are obtained for increasing values of the Grashof number and the wall temperature ratio especially in the wider passage. The effect of the viscoelastic parameter reduces the main velocity. As λx increases, the main velocity decreases at the wavy wall and remains constant at the flat wall. The effects of the Grashof number, wall temperature ratio, viscoelastic parameter, and λx are exactly opposite to their effect on the main velocity.
2. The temperature profiles remain invarient with changes in the Grashof number and the viscoelastic parameter at all baffle positions. The effect of the wall temperature ratio promotes the temperature whereas λx reduces the temperature at the wavy wall while it remains constant at the flat wall. Again, these effects are more pronounced in the wider passage than in the narrower passage.
3. The skin friction increases at the wavy wall and decreases at the flat wall for increasing values of the Grashof number and the wall temperature ratio. The viscoelastic parameter, wave number and the amplitude parameter reduce the skin friction at the wavy wall and do not vary it at the flat wall.
4. The increases in the Grashof number and the wall temperature ratio enhance the Nusselt number at the wavy wall and reduce it at the flat wall. The wave number decreases the Nusselt number at the wavy wall while it remains constant at the flat wall. The amplitude parameter reduces the rate of heat transfer at both channel walls.

ACKNOWLEDGEMENTS: The authors thank UGC-New Delhi for the financial support under UGC-Major Research Project.

6. REFERENCE

[1] K. Vajravelu, K.S. Sastri, Free convective heat transfer in a viscous incompressible fluid confined between a long vertical wavy wall and a parallel flat wall, *J. Fluid Mech.,* vol. 86, pp. 365-383, 1978

[2] K. Vajravelu, Combined free and forced convection in hydromagnetic flows in vertical wavy channels with traveling thermal waves, *Int. J. Engg. Sci.,* vol. 30, pp. 278-289, 1989.

[3] M.S. Malashetty, J.C. Umavathi, V. Leela, Magnetoconvective flow and heat transfer between vertical wavy wall and a parallel flat wall, *Int. J. Appl. Mech. Engg.,* vol. 6(2), pp. 437-456, 2001.

[4] S. Srinivas, R. Muthuraj, MHD flow with slip effects and temperature-dependent heat source in a vertical wavy porous space, *Chem. Eng. Comm.* vol. 197, pp.1387-1403, 2010.

[5] B.V. Rathish Kumar, P. Sing, P.V.S.N. Murthy, Effect of surface undulations on natural convection in a porous surface cavity, *ASME J. Heat Transfer,* vol. 119, pp. 848-851, 1997.

[6] B.V. Rathish Kumar, P.V.S.N. Murthy, P. Sing, Free convection heat transfer from an isothermal wavy surface in a porous enclosure, *Int. J. Numer. Mech. Fluids,* vol. 28, pp. 633-661, 1998.

[7] P.V.S.N. Murthy, B.V. Rathish Kumar, P. Sing, Natural convection heat transfer from a horizontal wavy surface in a porous enclosure, *Numer. Heat Transfer Part A,* vol. 31, pp. 202-221, 1997.

[8] B.V. Rathish Kumar, Shalini, Free convection in a non-Darcian wavy porous enclosure. *Int. J. Engg. Sci.* vol. 41**,** pp. 1827-1848, 2003.

[9] J.E. Dunn, K.R. Rajagopal, Fluids of different type: critical review and thermodynamic analysis, *Int. . Eng. Sci.,* vol. 33, pp. 689-729, 1995.

[10] K.R. Rajagopal, Mechanics of non-Newtonian Fluids, in : G.P. Galdi, J. Necas (Eds.), Recent Developments in Theoretical Fluid Mechanics, Pitman Research Notes in Mathematics, vol. 291, Longman, New York, 1993.

[11] Z.Y. Guo, B.X. Wang, A novel concept for convective heat transfer enhancement. *Int. J. Heat Mass Transfer,* vol. 41, pp. 2221-2225, 1998.

[12] W. Aung, L.S. Fletcher, V. Sernas, Developing laminar free convection between vertical flat plates with asymmetric heating, *Int. J. Heat Mass Transfer,* vol. 15, pp. 2293-2308, 1972.

[13] W. Aung, Fully developed laminar free convection between vertical flat plates heated asymmetrically, *Int. J. Heat Mass Transfer,* vol. 15, pp. 1577-1580, 1972.

[14] L. S. Yao, Free and forced convection between in the entry region of a heated vertical channel, *Int. J. Heat Mass Transfer,* vol. 26, pp. 65-72, 1983.

[15] W. Aung, G. Worku, Developing flow and flow reversal in mixed convection in a vertical channel with asymmetric wall temperatures, *Int. J. Heat Mass Transfer,* vol. 108, pp. 299-304, 1986.

[16] W. Aung, G. Worku, Theory of fully developed combined convection including flow reversal, *J. Heat Transfer,* vol. 108, pp. 485-488, 1986.

[17] M.M. Salah El-Din, Developing laminar convection in a vertical double passage channel*, Heat Mass Transfer,* vol. 38, pp. 93-96, 2001.

[18] R. Choudhury, A. Das, Free convection flow of a non-Newtonian fluid in a vertical channel, *Defence Science Journal,* vol. 50, pp. 37-44, 2000.

[19] S. Asghar, Masood Khan, T. Hayat, Magnetohydrodynamic transient flows of a non-Newtonian fluid, *Int. J. Non-Linear Mechanics,* vol. 40, pp. 589-601, 2005.

[20] A. Misirlioglu, A.C. Baytas, I. Pop, Free convection in a vertical cavity filled with a porous medium, *Int. J. Heat Mass Transfer,* vol. 48, pp. 1840-1850, 2005.

[21] C.H. Cheng, H.S. Kuo, W.H. Huang, Laminar fully developed forced-convection flow within an asymmetric heated horizontal double-passage channel, *Appl. Energy*, vol. 33, pp. 265-286, 1989.

[22] M.M. Salah El-Din, Fully developed laminar convection in a vertical double-passage channel,
Appl. Energy, vol. 47, pp. 69-75, 1994.

[23] M.M. Salah El-Din, Effect of viscous dissipation on fully developed laminar mixed convection in a vertical double-passage channel, *Int. J. Therm. Sci* , vol. 41, pp. 253-259, 2002.

[24] K. Walters, The motion of an elastico-viscous liquid contained between coaxial cylinders (II), *Quart. J. Mech. Appl. Maths,* vol. 13, pp. 444-461, 1960.

[25] K. Walters, The solution of flow problems in the case of materials with memories, *Journal of Mecanique*, vol. 1, pp. 474-478, 1962.

[26] R. Choudhury, A. Das, Free convection flow of a Non-Newtonian fluid in a vertical channel, *Defense*
Science Journal, vol. 50, pp. 37-44, 2000.

[27] S. Ostrach, An analysis of laminar free-convection flow and heat transfer about a flat plate parallel to the direction of the generating body force, *NACA, TN-2635*, Accession number-93R12788

[28] W. Aung, G. Worku, Theory of fully developed, combined convection including flow reversal, *J. of Heat Transfer,* vol. 108, pp. 485-488, 1986.

Nomenclature

d	channel width (m)
d^*	width of passage 1 (m)
c_p	dimensionless specific heat at constant pressure
g_x	acceleration due to gravity $\left(\mathrm{ms}^{-2}\right)$
G	Grashof number $\left(d^3 g_x \beta \left(T_w - T_s\right)/\nu^2\right)$
K	dimensionless viscoelastic parameter
k	wavelength (m)
Nu	Nusselt number

$\bar{p}$	pressure $\left(\mathrm{Nm^{-2}}\right)$
p	dimensionless pressure
P	Prandtl number $\left(c_p \eta_0 / k\right)$
p_s	static pressure $\left(\mathrm{Nm^{-2}}\right)$
rp	real part
i p	imaginary part
T	temperature $\left(\mathrm{K}\right)$
T_s	static temperature $\left(\mathrm{K}\right)$
U, V	velocities along X and Y directions $\left(\mathrm{ms^{-1}}\right)$
u, v	dimensionless velocities
X, Y	space co-ordinates $\left(\mathrm{m}\right)$
x, y	dimensionless space co-ordinates

Greek Symbols

β	dimensionless co-efficient of thermal expansion
ε	non-dimensional amplitude parameter $\left(\varepsilon^* / d\right)$
ε^*	amplitude $\left(\mathrm{m}\right)$
λ	non-dimensional wave number $\left(k / d\right)$
μ	viscosity $\left(\mathrm{kg\,m^{-1}\,s^{-1}}\right)$
ν	kinematic viscosity
θ	dimensionless temperature
ρ	density $\left(\mathrm{kg\,m^{-3}}\right)$
ρ_0	static density $\left(\mathrm{kg\,m^{-3}}\right)$
σ_{xy}	skin friction
ψ	stream function

Subscripts

i refer quantities for the fluids in stream 1 and stream 2, respectively.